Transfer Function Approximations for a New Class of Bandpass Distributed Network Structures

M. E. MOKARI-BOLHASSAN, MEMBER, IEEE, AND WALTER H. KU, MEMBER, IEEE

Abstract—**Characteristic functions for a new class of prototype bandpass transmission-line structures have been derived for both the maximally flat and equiripple or Chebyshev characteristics. The class of bandpass distributed structures considered in this paper consists of commensurate transmission lines with constraints in the form of a shunt open-circuited stub and/or a series short-circuited stub. The gain-bandwidth restrictions imposed by the reactance constraints have been derived and some explicit results are presented for the synthesis of this class of bandpass transmission-line networks. Results presented in this paper are directly applicable to the design of broad-band microwave passive and active networks. In particular, the results are applied to the design of broad-band matching networks for octave-band GaAs FET amplifiers.**

I. Introduction

IN BOTH passive and active microwave circuit designs, we often encounter the problem of broad-band matching of complex loads with prescribed reactive constraints. Specific examples include the broad-band matching of microwave antennas, the design of broad-band bipolar and FET amplifiers [1]–[3], and the broad-band coupling to high-Q resonant loads and circulators [4], [5]. In order to be able to absorb the reactive part of the load admittances, different circuit configurations are often needed. The general distributed network configuration shown in Fig. 1 has great flexibility and is useful for a number of broad-band matching applications especially for the design of broad-band bipolar and GaAs FET amplifiers.

Based on the circuit configuration shown in Fig. 1, characteristic functions for a new class of prototype bandpass transmission-line structures have been derived in this paper for both the maximally flat and equiripple or Chebyshev characteristics. The new class of prototype characteristics developed has great flexibility in adjusting the number of zeros of transmission at the origin and at infinity and the commensurate line length is one-eighth the wavelength at the center of the band. Having a relatively short transmission-line length and zeros of transmission both at the origin and infinity makes the new prototype useful for broad-band matching of complex impedances since the structure will contain both open-circuited and short-circuited stubs.

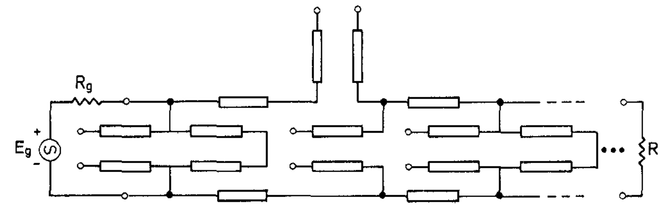

Fig. 1. A prototype of bandpass distributed structures.

The reactance constraints are represented in the form of a shunt open-circuited stub and/or a series short-circuited stub. The gain-bandwidth restrictions imposed by these reactance constraints have been derived and some explicit results for the synthesis of this class of bandpass transmission-line networks are presented in this paper. For octave-band applications, results for broad-band designs using five different circuit configurations are tabulated in terms of the gain factor K and the ripple parameter ε. Gain-bandwidth limitations are obtained for two different load constraints encountered in the design of the output matching networks for microwave chip and packaged FET amplifiers. These results are compared with the optimal limitations obtained for the ideal gain characteristics.

A characteristic function realizable in the form of Fig. 1 is given by [6]–[11]

$$|s_{12}|^2 = \frac{K\Omega^{2m}(1+\Omega^2)^n}{P_{n+m+r}(\Omega^2)} \leq 1 \qquad (1)$$

which has m zeros of transmission at $\Omega = 0$, r zeros of transmission at $\Omega = \infty$, and n cascaded lines. In (1), K is the gain parameter and P_{n+m+r} is a polynomial of order $n+m+r$ in Ω^2. If we use the transformation,

$$\Omega = \tan\theta$$
$$x = \alpha\cos\theta \qquad (2)$$

the gain function (1) reduces to

$$|s_{12}|^2 = \frac{K}{1 + \dfrac{H_{n+m+r}(x^2)}{(\alpha^2 - x^2)^m x^{2r}}} \qquad (3)$$

where the zeros at the origin are mapped to $x = \alpha$ and the zeros at infinity are mapped to $x = 0$. It is easy in general to make an approximation to (3) in the equiripple or Chebyshev sense if $r = 0$, but the solution is now known where r or m is not zero.

The frequency response of (3) repeats itself after each $\pi/2$ radians and there are no clear cutoff frequency points as can

Manuscript received June 23, 1975; revised April 14, 1977. This work was supported in part by the National Science Foundation under Grant GK-31012X and in part by the Rome Air Development Center, Air Force Systems Command, under Contract F30602-72-C-0497.

M. E. Mokari-Bolhassan is with the School of Electrical Engineering, Cornell University, Ithaca, NY, on leave from the Department of Electrical Engineering, Pahlavi University, Shiraz, Iran.

W. H. Ku is with the School of Electrical Engineering, Cornell University, Ithaca, NY 14853.

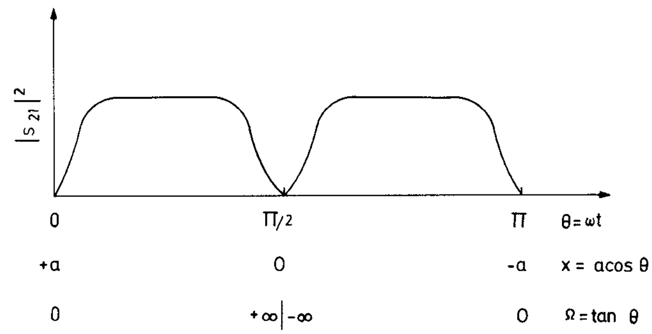

Fig. 2. The characteristic response of the prototype corresponding to (3).

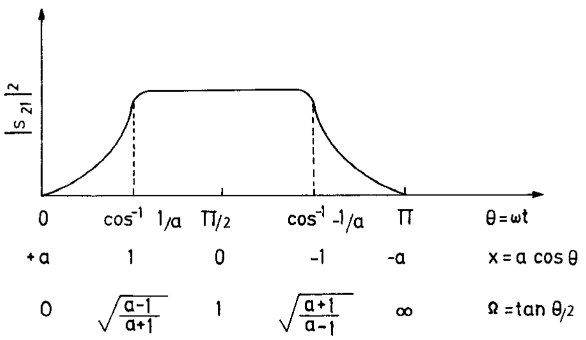

Fig. 3. The characteristic response of the prototype corresponding to (6).

be seen from Fig. 2. But if we use the transformations given in (4), we obtain a more standard form of characteristics versus x as is shown in Fig. 3. The characteristics repeat after each π radians. The new set of transformations are

$$\Omega = \tan \theta/2$$

$$x = \alpha \cos \theta \tag{4}$$

or

$$\Omega^2 = \frac{\alpha - x}{\alpha + x}. \tag{5}$$

Substituting (5) in (1), the results are

$$\begin{aligned} |s_{12}|^2 &= \frac{K\left(\frac{\alpha - x}{\alpha + x}\right)^m\left(\frac{2\alpha}{\alpha + x}\right)^n}{P_{n+m+r}\left(\frac{\alpha - x}{\alpha + x}\right)} \\ &= \frac{K(2\alpha)^n(\alpha - x)^m(\alpha + x)^r}{(\alpha + x)^{n+m+r}P_{n+r+m}\left(\frac{\alpha - x}{\alpha + x}\right)} \\ &= \frac{K(2\alpha)^n(\alpha - x)^m(\alpha + x)^r}{Q_{n+m+r}(\alpha - x)} \\ &= \frac{1}{1 + \frac{H_{n+m+r}(x)}{(\alpha - x)^m(\alpha + x)^r}}. \end{aligned} \tag{6}$$

The return loss of the bandpass structure of Fig. 1, P_{BP}, is given by

$$K \cdot P_{BP} = 1 + \frac{H_{n+m+r}(x)}{(\alpha - x)^m(\alpha + x)^r} \tag{7}$$

where the zeros at the origin are mapped to $x = \alpha$ and the zeros at infinity are mapped to $x = -\alpha$. Now even for the Chebyshev case we will be able to approximate (7) if $n + m + r$ is an even number. It will be shown subsequently that to make (7) maximally flat or equiripple $n + m + r$ must be even. Note that the commensurate transmission lines will be one-eighth wavelength long at $(F_H + F_L)/2$, where F_H and F_L are, respectively, the high and low end of the frequency band.

II. Butterworth Approximation

We shall rewrite (7) as

$$K \cdot P_{BP} = 1 + (10^{\alpha_m/10} - 1) \cdot \frac{C_{n+m+r}x^{n+m+r} + C_{n+m+r-1}x^{n+m+r-1} + \cdots}{(\alpha - x)^m(\alpha + x)^r}. \tag{8}$$

Although the function does seem to be even, the gain function will be even if $n + m + r$ is even. To make (8) maximally flat around $x = \beta$ we need to set

$$\frac{\partial^i P_{BP}}{(\partial x)^i} = 0, \qquad i = 0, 1, \cdots, \quad n + m + r - 1 \tag{9}$$

at $x = \beta$, center of the passband. This leads to

$$K \cdot P_{BP} = 1 + \frac{\varepsilon^2 A^2 (x - \beta)^{n+m+r}}{(\alpha - x)^m(\alpha + x)^r}. \tag{10}$$

A is determined from band-edge requirements; i.e., for $\beta = 0$ and band edge $x = \pm 1$ (Fig. 3) if we require that $10 \log P_{BP} = \alpha_m$ dB at $x = +1$ the result will be

$$A^2 = (\alpha - 1)^m(\alpha + 1)^r. \tag{11}$$

The attenuation on the other band edge may be determined from (10). Transforming (10) back to the Ω domain by using

$$x = \alpha \frac{1 - \Omega^2}{1 + \Omega^2} \tag{12}$$

we obtain

$$|s_{12}|^2 = \frac{K\Omega^{2m}(1 + \Omega^2)^n}{\Omega^{2m}(1 + \Omega^2)^n + \eta^2(1 - \Omega^2)^{n+m+r}} \tag{13}$$

where

$$\eta^2 = \varepsilon^2 \frac{\alpha^n(\alpha - 1)^m(\alpha + 1)^r}{2^{m+r}}. \tag{14}$$

III. Chebyshev Approximation

We may rewrite (6) as

$$|s_{12}|^2 = \frac{K}{1 + \varepsilon_1^2 F(x)}. \tag{15}$$

It is easy to show that the response will be equiripple between $x = a$ and $x = b$ if [6]–[10]

$$F(x) = 1 + \cos(n\phi + m\xi_1 + r\xi_2) \tag{16}$$

where

$$\cos\phi = \frac{2x-(a+b)}{a-b} \quad (17a)$$

$$\cos\xi_1 = \frac{x(a+b-2\alpha)+\alpha(a+b)-2ab}{(a-b)(x-\alpha)} \quad (17b)$$

$$\cos\xi_2 = \frac{x(a+b+2\alpha)-\alpha(a+b)-2ab}{(a-b)(x+\alpha)}. \quad (17c)$$

In order for $|s_{12}|^2$ to be an even rational function in Ω, $n+m+r$ must be an even number. To show this let $x=a=+1$ and $x=b=-1$, then (17) reduces to

$$\cos\phi = x = \alpha\cos\theta \quad (18)$$

and

$$\cos\xi_1 = \frac{\alpha x-1}{\alpha - x}$$

$$\cos\xi_2 = \frac{\alpha x+1}{\alpha + x}. \quad (19)$$

substituting this in (16) leads to

$$F(x) = 1+\cos(n\phi)\cos(m\xi_1+r\xi_2) - \sin\phi n\sin(m\xi_1+r\xi_2) \quad (20)$$

where

$$\cos(n\phi) = T_n(x) \quad (21)$$

and

$$\sin(n\phi) = \sqrt{1-x^2}\,Q_n(x) \quad (22)$$

where $T_n(x)$ is a Chebyshev polynomial of degree n and $Q_n(x)$ is a rational polynomial of degree n [6]–[10]. To show that (19) is rational we proceed as follows:

$$\cos(m\xi_1+r\xi_2) = \cos(m\xi_1)\cos r\xi_2 - \sin m\xi_1 \sin r\xi_2 \quad (23a)$$

$$\sin(m\xi_1+r\xi_2) = \sin m\xi_1\cos r\xi_2 + \cos m\xi_1 \sin r\xi_2 \quad (23b)$$

$$\cos m\xi_1 = 2\cos(m-1)\xi_1\cos\xi_1 - \cos(m-2)\xi_1 \quad (23c)$$

$$\sin m\xi_1 = 2\sin(m-1)\xi_1\cos\xi_1 - \sin(m-2)\xi_1. \quad (23d)$$

It is clear that $\cos m\xi_1$ and $\cos r\xi_2$ are rational functions of x. The terms $\sin m\xi_1$ and $\sin r\xi_2$ are multiplications of the $\sqrt{1-x^2}$ term and a rational function of x (see (23d)). Substituting these in (16) it is easy to see that the result is a rational function of x. To make the function even in terms of x and Ω, $n+m+r$ has to be constrained to be even number.

For $n=1$, $m=2$, and $r=1$ (i.e., one cascaded line and three stubs; two zeros of transmission at the origin and one zero of transmission at infinity), the characteristic function is given by

$$|s_{12}|^2 = \frac{K8\alpha^3\Omega^4(1+\Omega^2)}{C_0+C_1\Omega^2+C_2\Omega^4+C_3\Omega^6+C_4\Omega^8} \quad (24)$$

where

$$\begin{aligned}
C_0 &= \varepsilon_1^2[\sqrt{\alpha^2-1}\,(4\alpha^6-8\alpha^4+4\alpha^2)+4\alpha^7-8\alpha^5+4\alpha^3]\\
C_1 &= \varepsilon_1^2[\sqrt{\alpha^2-1}\,(-16\alpha^6+8\alpha^4-8\alpha^2)-16\alpha^7+16\alpha^5]\\
C_2 &= 8\alpha^3+\varepsilon_1^2[\sqrt{\alpha^2-1}\,(24\alpha^6+4\alpha^4+4\alpha^2)\\
&\quad +24\alpha^7-12\alpha^5+4\alpha^3]\\
C_3 &= 8\alpha^3+\varepsilon_1^2[\sqrt{\alpha^2-1}\,(-16\alpha^6)-16\alpha^7+8\alpha^5+8\alpha^3]\\
C_4 &= \varepsilon_1^2[\sqrt{\alpha^2-1}\,(4\alpha^6-4\alpha^4)+4\alpha^7-4\alpha^5].
\end{aligned} \quad (25)$$

This function has the required form and may be synthesized to yield element values for different K and ε_1.

For special cases where n is even and $m=r$, (16) may be written in the following form

$$|s_{12}|^2 = \frac{K}{1+\varepsilon^2\cos^2\left[\frac{n}{2}\phi+m\xi\right]} \quad (26)$$

where

$$\cos\xi = x\sqrt{\frac{\alpha^2-1}{\alpha^2-x^2}} \quad (27)$$

and

$$\varepsilon^2 = 2\varepsilon_1^2. \quad (28)$$

For this case, let $n=0$ and $m=1$, the characteristic function is obtained as

$$|s_{12}|^2 = \frac{2K\Omega^2}{2\Omega^2+\varepsilon^2(\alpha^2-1)(1-\Omega^2)^2} \quad (29)$$

which has the required form.

For $n=2$ and $m=1$, we have for $\cos^2(\phi+\xi)$

$$\cos^2(\phi+\xi) = \frac{\begin{aligned}&\{\Omega^8[\alpha^2(\sqrt{\alpha^2-1}+\alpha)^2+1.0-2\alpha(\sqrt{\alpha^2-1}+\alpha)]+\Omega^6[-4\alpha^2(\sqrt{\alpha^2-1}+\alpha)^2+4]\\&+\Omega^4[6\alpha^2(\sqrt{\alpha^2-1}+\alpha)^2+6+4\alpha(\sqrt{\alpha^2-1}+\alpha)]+\Omega^2[-4\alpha^2(\sqrt{\alpha^2-1}+\alpha)^2+4]\\&+[\alpha^2(\sqrt{\alpha^2-1}+\alpha)^2+1-2\alpha(\sqrt{\alpha^2-1}+\alpha)]\}\end{aligned}}{4\Omega^2(1+\Omega^2)^2} = \frac{N}{D} \quad (30)$$

and

$$|s_{12}|^2 = \frac{K}{1+\varepsilon^2\cos^2(\phi+\xi)} = \frac{4K\alpha^2\Omega^2(1+\Omega^2)^2}{3\alpha^2\Omega^2(1+\Omega^2)^2+\varepsilon^2 N} \quad (31)$$

TABLE I
ELEMENT VALUES FOR THE CHEBYSHEV FUNCTION, $n = 2$, $m = 1$, $r = 1$, $\alpha = 2$, AND $R_g = 1.0\ \Omega$

		Ripple Parameter ϵ^2					
K		0.01	0.04	0.09	0.16	0.25	0.36
0.80	Z_{01}	1.0191	0.6125	0.4695	0.3908	0.3382	0.2991
	Z_{02}	0.3122	0.2825	0.2585	0.2371	0.2177	0.2002
	Z_{03}	0.1658	0.1042	0.0749	0.0581	0.0472	0.0396
	Z_{04}	0.5410	0.2258	0.1361	0.0957	0.07330	0.0592
	R_L	0.1529	0.1065	0.0870	0.0766	0.0702	0.0659
0.85	Z_{01}	1.1443	0.6919	0.5310	0.4414	0.3811	0.3363
	Z_{02}	0.3606	0.3255	0.2965	0.2705	0.2472	0.2265
	Z_{03}	0.1878	0.1172	0.0840	0.6495	0.0527	0.0442
	Z_{04}	0.5959	0.2492	0.1505	0.1060	0.0812	0.0656
	R_L	0.1746	0.1221	0.1002	0.0883	0.0811	0.0762
0.90	Z_{01}	1.3011	0.7924	0.6082	0.5043	0.4341	0.3819
	Z_{02}	0.4241	0.3813	0.3449	0.3125	0.2839	0.2588
	Z_{03}	0.2156	0.1335	0.0953	0.0734	0.0594	0.0497
	Z_{04}	0.6614	0.2776	0.1680	0.1184	0.0908	0.0734
	R_L	0.2031	0.1431	0.1179	0.1042	0.0957	0.0900
0.95	Z_{01}	1.5251	0.9365	0.7168	0.5913	0.5062	0.4434
	Z_{02}	0.5199	0.4634	0.4140	0.3710	0.3341	0.3025
	Z_{03}	0.2555	0.1566	0.1109	0.0849	0.0684	0.0571
	Z_{04}	0.7497	0.3165	0.1919	0.1354	0.1037	0.0838
	R_L	0.2472	0.1762	0.1458	0.1289	0.1183	0.1111
1.00	Z_{01}	2.2789	1.3662	1.0165	0.8205	0.6915	0.5987
	Z_{02}	0.8411	0.7030	0.6004	0.5222	0.4608	0.4114
	Z_{03}	0.3876	0.2253	0.1545	0.1160	0.0922	0.0763
	Z_{04}	1.0502	0.4379	0.2616	0.1823	0.1384	0.1110
	R_L	0.4608	0.3205	0.2574	0.2222	0.2002	0.1855

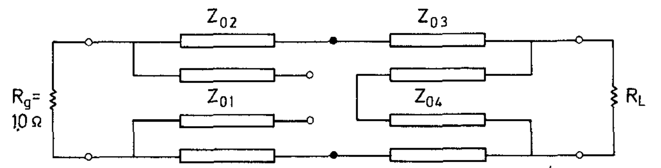

Fig. 4. Circuit realization useful in output matching chip FET amplifiers; Chebyshev function with $n = 2$, $m = r = 1$, and $\alpha = 2$.

or specifically

$$|s_{12}|^2 = \frac{4K\Omega^2(1+\Omega^2)^2}{\{\Omega^8[\alpha^2(\sqrt{\alpha^2-1}+\alpha)^2 + 1.0 - 2\alpha(\sqrt{\alpha^2-1}+\alpha)]\varepsilon^2 + \Omega^6\{[-4\alpha^2(\sqrt{\alpha^2-1}+\alpha)^2+4]\varepsilon^2+4\} + \Omega^4\{[6\alpha^2(\sqrt{\alpha^2-1}+\alpha)^2 + 6 + 4\alpha(\sqrt{\alpha^2-1}+\alpha)]\varepsilon^2 + 8\} + \Omega^2\{[-4\alpha^2(\sqrt{\alpha^2-1}+\alpha)^2+4]\varepsilon^2+4\} + [\alpha^2(\sqrt{\alpha^2-1}+\alpha) + 1.0 - 2(\sqrt{\alpha^2-1}+\alpha)]\varepsilon^2\}}. \quad (32)$$

This function is synthesized for different K and ε and the configuration given in Fig. 4. The results are tabulated in Table I. This configuration is useful in output matching chip FET amplifiers [1]–[3]. For the packaged FET's the configurations given in Figs. 5 and 6 are required. To realize the circuit of Fig. 5, we use the Butterworth functions of (15) with $n = 1$, $m = 1$, and $r = 2$. The element values are tabulated in Table II. We have chosen $n = 2$ and $m = r = 2$ in the Chebyshev function of (17) for the configuration of Fig. 6. The synthesized results are presented in Table III. Two other tables are presented for completeness and further usage. The elements for the Chebyshev function with $n = 1$, $m = 2$, $r = 1$, and $\alpha = 2$ are given in Table IV and the elements' values for $n = 1$, $m = 1$, $r = 2$, and $\alpha = 2$ are given in Table V.

IV. GAIN-BANDWIDTH LIMITATIONS

In this section, the gain-bandwidth restrictions are applied to the reactively constrained loads given in Fig. 7(a) and (b), which correspond to the output circuit models of a microwave chip and packaged FET, respectively [1]–[3]. These loads can be matched using the configurations given in Figs. 4–6.

TABLE II
ELEMENT VALUES FOR THE BUTTERWORTH FUNCTION, $n = 1$, $m = 1$, $r = 2$, $\alpha = 2$, AND $R_g = 1.0\ \Omega$

		Ripple Parameter ϵ^2					
K		0.01	0.04	0.09	0.16	0.25	0.36
0.80	Z_{01}	0.66516	0.48296	0.39948	0.34865	0.31345	0.28719
	Z_{02}	0.12030	0.14958	0.16144	0.16594	0.16689	0.16598
	Z_{03}	1.75313	0.83238	0.52833	0.37827	0.29001	0.23219
	Z_{04}	0.31707	0.25781	0.21351	0.18012	0.15441	0.13419
	R_L	0.34576	0.31178	0.28263	0.25777	0.23655	0.21834
0.85	Z_{01}	0.76021	0.55172	0.45618	0.39803	0.35778	0.32776
	Z_{02}	0.14220	0.17564	0.18869	0.19332	0.19392	0.19248
	Z_{03}	1.94020	0.92020	0.58348	0.41754	0.31973	0.25580
	Z_{04}	0.36292	0.29295	0.24134	0.20279	0.17330	0.15022
	R_L	0.39857	0.35863	0.32442	0.29535	0.27060	0.24942
0.90	Z_{01}	0.88386	0.64100	0.52973	0.46204	0.41521	0.38030
	Z_{02}	0.17220	0.21088	0.22525	0.22982	0.22984	0.22758
	Z_{03}	2.16198	1.02441	0.64888	0.46389	0.35492	0.28374
	Z_{04}	0.42123	0.33701	0.27591	0.23074	0.19646	0.16979
	R_L	0.46742	0.41977	0.37894	0.34431	0.31491	0.28982
0.95	Z_{01}	1.06993	0.77498	0.63994	0.55786	0.50113	0.45887
	Z_{02}	0.21998	0.26603	0.28191	0.28605	0.28489	0.28120
	Z_{03}	2.45308	1.16203	0.73546	0.52531	0.40156	0.32078
	Z_{04}	0.50437	0.39890	0.32399	0.26936	0.22829	0.19657
	R_L	0.57009	0.51169	0.46119	0.41829	0.38192	0.35094
0.98	Z_{01}	1.27354	0.92100	0.75981	0.66198	0.59442	0.54414
	Z_{02}	0.27446	0.32781	0.34480	0.34811	0.34544	0.34002
	Z_{03}	2.71964	1.29048	0.81707	0.58355	0.44597	0.35614
	Z_{04}	0.58611	0.45931	0.37078	0.30687	0.25917	0.22254
	R_L	0.67926	0.61176	0.55180	0.50037	0.45663	0.41934

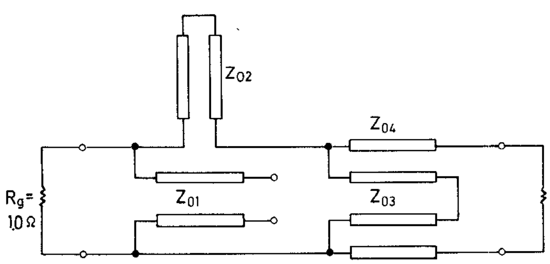

Fig. 5. Circuit realization useful in output matching packaged FET amplifiers; Butterworth function with $n = 1$, $m = 1$, $r = 2$, and $\alpha = 2$.

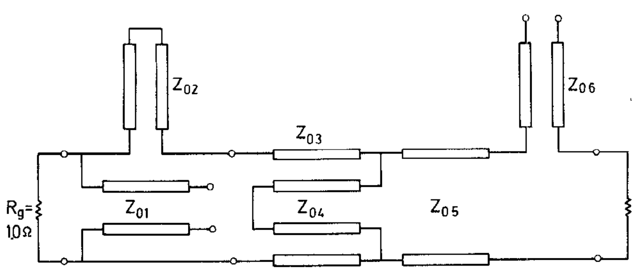

Fig. 6. Circuit realization useful in output matching packaged FET amplifiers; Chebyshev function with $n = 2$, $m = r = 2$, and $\alpha = 2$.

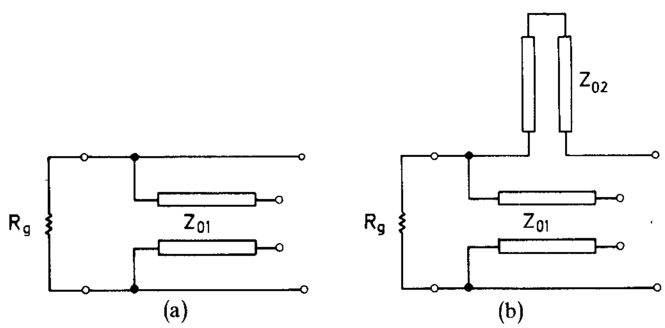

Fig. 7. (a) and (b) Reactive constraint load.

A. Simple Low-Pass Constraint

The integral constraint for the load of Fig. 7(a) is given by [13], [14]

$$\int_0^\infty \ln \frac{1}{|s_{11}(j\Omega)|^2}\, d\Omega < \frac{2\pi}{\tau} \tag{33}$$

where $\tau = R_g/Z_{01}$. It is easy to apply this to an idealized gain function defined by

$$|s_{12}(j\Omega)|^2 = \begin{cases} K, & \text{for } \sqrt{\dfrac{\alpha-1}{\alpha+1}} < \Omega < \sqrt{\dfrac{\alpha+1}{\alpha-1}} \\ 0, & \text{elsewhere.} \end{cases} \tag{34}$$

TABLE III
ELEMENT VALUES FOR THE CHEBYSHEV FUNCTION,
$n = 2$, $m = 2$, $r = 2$, $\alpha = 2$, AND $R_g = 1.0\ \Omega$

		Ripple Parameter ϵ^2					
K		0.01	0.04	0.09	0.16	0.25	0.36
0.80	Z_{01}	0.45932	0.37355	0.32842	0.29533	0.26817	0.24498
	Z_{02}	0.17064	0.18183	0.17814	0.16968	0.15959	0.14922
	Z_{03}	0.12566	0.08570	0.06745	0.05641	0.04873	0.04296
	Z_{04}	0.16302	0.10601	0.08284	0.06924	0.05985	0.05280
	Z_{05}	0.20299	0.19081	0.18556	0.17983	0.17276	0.16473
	Z_{06}	0.09783	0.11489	0.12361	0.12682	0.12627	0.12331
	R_L	0.22985	0.18739	0.15790	0.13382	0.11361	0.09670
0.85	Z_{01}	0.53043	0.43096	0.37733	0.33760	0.30510	0.27757
	Z_{02}	0.20025	0.21153	0.20563	0.19452	0.18189	0.16927
	Z_{03}	0.14332	0.09769	0.07675	0.06402	0.05514	0.04847
	Z_{04}	0.18685	0.12174	0.09494	0.07907	0.06807	0.05983
	Z_{05}	0.23834	0.22493	0.21803	0.20996	0.20031	0.18977
	Z_{06}	0.11731	0.13758	0.14697	0.14942	0.14743	0.14283
	R_L	0.26728	0.21650	0.18055	0.15134	0.12721	0.10735
0.90	Z_{01}	0.62570	0.50691	0.44069	0.39134	0.35134	0.31791
	Z_{02}	0.240411	0.25078	0.24107	0.22590	0.20964	0.19394
	Z_{03}	0.16628	0.11326	0.08870	0.07366	0.06316	0.05530
	Z_{04}	0.21901	0.14287	0.11096	0.09179	0.07854	0.06866
	Z_{05}	0.28819	0.27293	0.26268	0.25035	0.23640	0.22197
	Z_{06}	0.14584	0.17032	0.17968	0.18009	0.17542	0.16813
	R_L	0.31839	0.25510	0.20934	0.17273	0.14325	0.11958
0.95	Z_{01}	0.77562	0.62239	0.53331	0.46753	0.41549	0.37304
	Z_{02}	0.303495	0.30951	0.29198	0.26969	0.24763	0.22729
	Z_{03}	0.20096	0.13654	0.10612	0.08736	0.07434	0.06470
	Z_{04}	0.27116	0.17634	0.13522	0.11048	0.09352	0.08106
	Z_{05}	0.37362	0.35323	0.33382	0.31192	0.28959	0.26824
	Z_{06}	0.19726	0.22685	0.23288	0.22754	0.21712	0.13436
	R_L	0.40106	0.31356	0.24976	0.20092	0.16338	0.13436
1.00	Z_{01}	1.40439	1.00232	0.80290	0.67526	0.58399	0.51457
	Z_{02}	0.52473	0.47967	0.42728	0.381353	0.34245	0.30956
	Z_{03}	0.33371	0.21372	0.15844	0.12610	0.10475	0.08955
	Z_{04}	0.54595	0.30894	0.21719	0.16780	0.13679	0.11546
	Z_{05}	0.85844	0.69338	0.58572	0.50746	0.44719	0.39911
	Z_{06}	0.52473	0.47967	0.42728	0.38135	0.34245	0.30956
	R_L	0.73692	0.48078	0.34306	0.25751	0.19998	0.15929

Substituting (34) in (33) and carrying out the integration result in the optimal gain-bandwidth limitation given by

$$K < 1 - \exp\{-\pi\sqrt{\alpha^2 - 1}\,(Z_{01}/R_g)\}. \tag{35}$$

Application of (33) to an actual gain function is not as easily accomplished. Instead we will use the equivalent coefficient relations derived by Youla [14]. It is necessary to factor $s_{11}(\lambda)s_{11}(-\lambda)$ in the λ domain when $j\Omega = \lambda$ is substituted in $|s_{11}(j\Omega)|^2$. The gain-bandwidth limitations in terms of maximum return loss versus ε are shown in Fig. 8(a) for the ideal case and the Chebyshev function of $n = 2$, $m = r = 1$ for different ε. This figure shows the nature of the tradeoff involved in gain versus reactive constraint and the ripple factor ε. Similar curves are obtained for the case of $n = 4$ and $m = r = 1$ and are shown in Fig. 8(b).

B. Double-Order Low-Pass Constraints

The integral constraints for the load given in Fig. 7(b) are obtained as [13], [14]

$$\int_0^{\infty} \ln \frac{1}{|s_{11}(j\Omega)|^2}\, d\Omega = \frac{2\pi Z_{01}}{R_g} \tag{36}$$

and

$$\frac{1}{\pi}\int_0^{\infty} \Omega^2 \ln \frac{1}{|s_{11}(j\Omega)|^2}\, d\Omega \le \frac{Z_{01}^2}{R_g Z_{02}} - \frac{1}{3}\left(\frac{Z_{01}}{R_g}\right)^3. \tag{37}$$

TABLE IV
ELEMENT VALUES FOR THE CHEBYSHEV FUNCTION, $n = 1$, $m = 2$, $r = 1$, $\alpha = 2$, AND $R_g = 1.0\ \Omega$

K		0.01	0.04	0.09	0.16	0.25	0.36
0.80	Z_{01}	1.6283	2.16842	2.58242	2.95731	3.32178	3.68708
	Z_{02}	7.28910	6.17581	6.02250	6.17289	6.47244	6.86199
	Z_{03}	4.35363	6.35365	8.46714	10.65925	12.90771	15.19693
	Z_{04}	16.87730	15.67126	17.10022	19.26852	21.78092	24.49368
	R_L	4.20642	6.81131	10.27499	14.63432	19.92522	26.17624
0.85	Z_{01}	1.42045	1.89345	2.26208	2.60042	2.93196	3.26529
	Z_{02}	6.18061	5.28913	5.20373	5.37560	5.67108	6.04299
	Z_{03}	3.83680	5.64180	7.55019	9.53092	11.56344	13.63318
	Z_{04}	14.45789	13.64831	15.04164	17.05960	19.36978	21.85036
	R_L	3.74068	6.16683	9.41017	13.50414	18.47971	24.36155
0.90	Z_{01}	1.21656	1.62557	1.95240	2.25757	2.55887	2.86239
	Z_{02}	5.11971	4.44338	4.42627	4.61876	4.91315	5.26827
	Z_{03}	3.34044	4.95694	6.66735	8.44526	10.27086	12.13037
	Z_{04}	12.17441	11.73307	13.09038	14.96330	17.07846	19.33503
	R_L	3.30479	5.57689	8.63172	12.49698	17.19808	22.75623
0.95	Z_{01}	0.99819	1.34351	1.63144	1.90562	2.17769	2.45156
	Z_{02}	4.02975	3.58364	3.64303	3.86021	4.15267	4.48977
	Z_{03}	2.82776	4.24652	5.75377	7.32347	8.93677	10.58050
	Z_{04}	9.88635	9.80949	11.12694	12.84757	14.75848	16.78106
	R_L	2.88112	5.03109	7.93349	11.60657	16.07080	21.34537
1.00	Z_{01}	0.59137	0.86931	1.11127	1.34379	1.57024	1.79545
	Z_{02}	2.29547	2.29045	2.47478	2.71927	2.99461	3.28996
	Z_{03}	1.98329	3.07415	4.24452	5.46897	6.73017	8.01637
	Z_{04}	6.66693	7.01458	8.17547	9.58424	11.11554	12.72111
	R_L	2.53034	4.66351	7.47668	11.00329	15.27030	20.2998

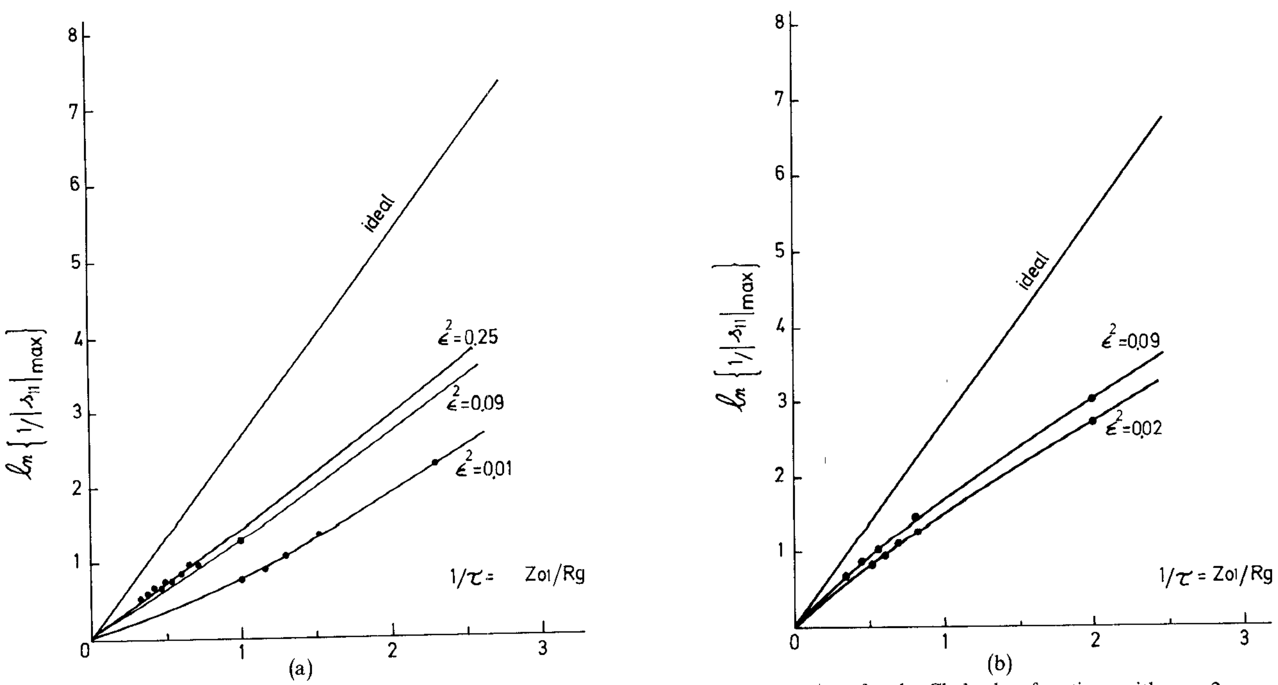

Fig. 8. (a) Maximum passband return loss versus time constant $\tau = R_g/Z_{01}$ for the Chebyshev functions with $n = 2$, $m = r = 1$, and $\alpha = 2$. (b) Maximum passband return loss versus time constant $\tau = R_g/Z_{01}$ for the Chebyshev function with $n = 4$, $m = r = 1$, and $\alpha = 2$.

TABLE V
ELEMENT VALUES FOR THE CHEBYSHEV FUNCTION, $n = 1$, $m = 1$, $r = 2$, $\alpha = 2$, AND $R_g = 1.0\ \Omega$

K		0.01	0.04	0.09	0.16	0.25	0.36
0.80	Z_{01}	0.72487	0.52990	0.43465	0.37124	0.32317	0.28441
	Z_{02}	0.11388	0.13983	0.14716	0.14597	0.14050	0.13294
	Z_{03}	1.50166	0.73006	0.47355	0.34542	0.26861	0.21746
	Z_{04}	0.31599	0.25802	0.21475	0.18192	0.15641	0.13614
	R_L	0.35655	0.33710	0.31913	0.30186	0.28521	0.26918
0.85	Z_{01}	0.82918	0.60470	0.49378	0.41940	0.36299	0.31768
	Z_{02}	0.13456	0.16363	0.17061	0.16772	0.16012	0.15041
	Z_{03}	1.66461	0.80930	0.52444	0.38190	0.29635	0.23938
	Z_{04}	0.36182	0.29331	0.24269	0.20456	0.17509	0.15179
	R_L	0.41236	0.38989	0.36837	0.34727	0.32675	0.30698
0.90	Z_{01}	0.96503	0.70061	0.56780	0.47813	0.41034	0.35639
	Z_{02}	0.16282	0.19525	0.20082	0.19494	0.18404	0.17121
	Z_{03}	1.85940	0.90415	0.58491	0.42474	0.32850	0.26442
	Z_{04}	0.42018	0.33748	0.27707	0.23195	0.19733	0.17014
	R_L	0.48593	0.45959	0.43276	0.40569	0.37918	0.35377
0.95	Z_{01}	1.16908	0.83918	0.66940	0.55489	0.46971	0.40328
	Z_{02}	0.20744	0.24258	0.24358	0.23160	0.21493	0.19717
	Z_{03}	2.11863	1.03013	0.66359	0.47899	0.36809	0.29447
	Z_{04}	0.5035	0.39883	0.32341	0.26777	0.22559	0.19283
	R_L	0.59767	0.56519	0.52770	0.48879	0.45103	0.41566
	Z_{01}	1.78078	1.14161	0.84985	0.67366	0.55320	0.46486
	Z_{02}	0.34406	0.34912	0.32267	0.29092	0.26038	0.23277
	Z_{03}	2.74789	1.28665	0.80137	0.56353	0.42455	0.33451
	Z_{04}	0.71109	0.52701	0.40753	0.32595	0.26764	0.22434
	R_L	0.95515	0.83763	0.73112	0.64274	0.57000	0.50957

For the ideal gain response of (34), these constraints become

$$K = 1 - \exp\left\{\frac{-\pi\sqrt{\alpha^2 - 1}\,Z_{01}}{R_g}\right\} \tag{38}$$

and

$$\frac{Z_{02}}{R_g} \le \frac{1}{\dfrac{Z_{01}}{3R_g} + \dfrac{R_g}{3Z_{01}}\left(\dfrac{3\alpha^2 + 1}{\alpha^2 - 1}\right)}. \tag{39}$$

It is clear from these relations that once the first or "inner" reactive constraint is satisfied exactly, there is a limit on the second constraint which will be achievable with a given gain function. For actual functions this restriction is still present, but the range will depend also on the ripple factor. Youla's coefficient constraint [14] is applied for the Chebyshev function of $n = 2$ and $m = r = 2$ with the required configuration to realize this load. The results using the equality sign are shown in Fig. 9.

The graphs of Figs. 8 and 9 may be used for matching lumped constrained loads by distributed lossless networks. Since the lines are relatively short, only one-eighth the wavelength at the center of the band, the open- and short-circuited stubs can be approximated by lumped capacitors and inductors, respectively [12]. The approximate values may be obtained from

$$C \simeq \frac{\tan\dfrac{\theta}{2}}{2\pi f_0 R_g Z_{01}} \tag{40}$$

and

$$L \simeq \frac{R_g \tan\dfrac{\theta}{2}}{2\pi f_0} Z_{02} \tag{41}$$

where f_0 is the center frequency at which $\theta/2 = 45°$ for this class of functions. If we normalize $2\pi f_0 \equiv 1$, we can read $\tau_1 = R_g C$ and $\tau_2 = L/R_g$ directly from Figs. (8) and (9) for the octave band. It has been found, in practice, that this comparison is very useful for obtaining an estimate on how well a certain load can be matched in the given band.

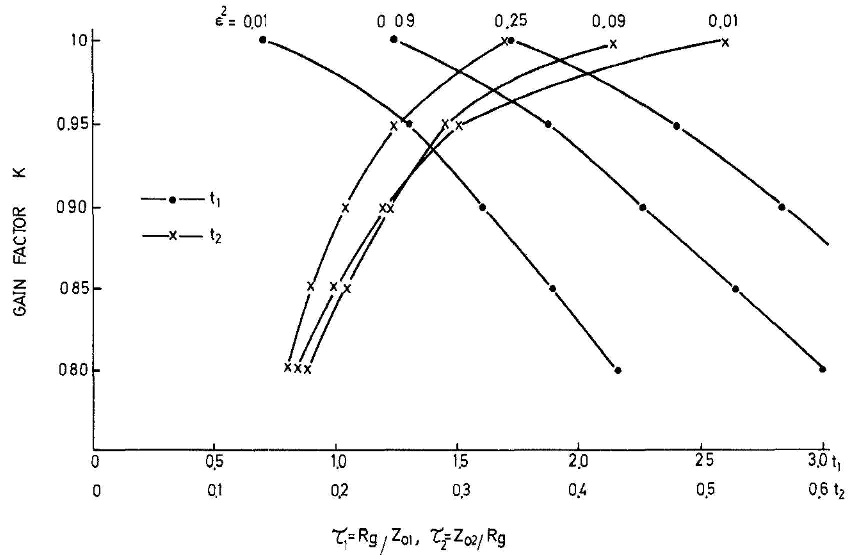

Fig. 9. Gain factor K versus time constants $\tau_1 = R_g/Z_{01}$ and $\tau_2 = Z_{02}/R_g$ for the Chebyshev function with $n = 2$, $m = r = 2$, and $\alpha = 2$.

TABLE VI
MEASURED s_{22} OF A 1-μ-GATE GaAs CHIP FET

	s_{22}	
FREQ (GHz)	MAG	ANGLE
7.0	0.834	- 19.3
7.5	0.832	- 20.4
8.0	0.830	- 21.4
8.5	0.829	- 22.5
9.0	0.828	- 23.6
9.5	0.827	- 24.7
10.0	0.826	- 25.7
10.5	0.826	- 26.8
11.0	0.826	- 27.8
11.5	0.826	- 28.9
12.0	0.826	- 29.9
12.5	0.826	- 30.9
13.0	0.827	- 31.9
13.5	0.828	- 33.0
14.0	0.829	- 34.0

V. EXAMPLES

In this section, we consider the broad-band matching of the output circuit of the GaAs FET amplifiers. In the first example the output matching circuit of a 1-μ-chip FET is designed for the 7–14-GHz band.

The second example is concerned with the design of the output matching network of a packaged FET to cover the 4–8-GHz frequency band [3].

A. 1-μ-Gate FET

The output of the chip FET can be modeled as an open-circuited stub in parallel with a resistor as shown in Fig. 7(a). The parameters of the model for measured s_{22} of the FET, tabulated in Table VI for 7–14 GHz, are obtained as

$$R_g = 497.5\ \Omega$$
$$Z_{01} = 236.2\ \Omega$$
$$l = \tfrac{1}{8} \text{ wavelength at 10.5 GHz.} \qquad (42)$$

Now for $\alpha = 2$ (octave bandwidth) and $\tau_1 = Z_{01}/R_g = 0.47477$, we can get an estimate from Table I corresponding to the configuration of Fig. 4. For $K = 0.95$, τ_1 can be realized exactly for a ripple factor between 0.25 and 0.36. It is found by a simple interpolation that $K = 0.95$ with $\varepsilon^2 = 0.3$ will absorb the reactive constraint exactly. From (17), with $n = 2$ and $m = r = 1$, the reflection function is given by

$$s_{11}(\lambda) = \frac{1 + 0.33939\lambda + 2.66838\lambda^2 + 0.33929\lambda^3 + \lambda^4}{1 + 1.28754\lambda + 3.28814\lambda^2 + 1.28754\lambda^3 + \lambda^4}. \qquad (43)$$

The synthesized circuit is given in Fig. 10 with its response shown in Fig. 11.

B. Packaged FET

The output of the packaged FET can be modeled with the configuration shown in Fig. 7(b). The element values for this model for the measured s_{22} of the FET, tabulated in Table VII for the 4–8-GHz band, are obtained as

$$R_g = 139.12\ \Omega$$
$$Z_{01} = 107.52\ \Omega$$
$$Z_{02} = 23.16\ \Omega$$
$$l = \tfrac{1}{8} \text{ wavelength at 6 GHz.} \qquad (44)$$

For $\alpha = 2$, $\tau_1 = 0.77286$, and $\tau_2 = 0.16647$, an estimate can be obtained from either Table II or Table III. From Table II, for the Butterworth function, we see that K between 0.95 and 1.0 and ε^2 approximately equal to 0.09 will

TABLE VII
MEASURED s_{22} OF A PACKAGED GaAs FET

FREQ (GHz)	s_{22}	
	MAG	ANGLE
4.0	0.563	- 42.4
4.5	0.520	- 47.9
5.0	0.485	- 55.8
5.5	0.457	- 64.0
6.0	0.412	- 74.7
6.5	0.370	- 83.3
7.0	0.320	- 95.9
7.5	0.266	-109.9
8.0	0.244	-132.0

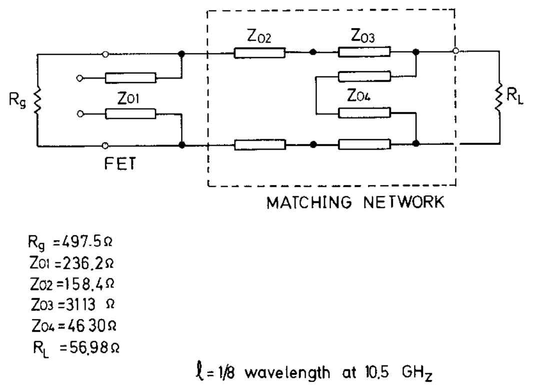

Fig. 10. Output matching network for a chip FET amplifier in the 7–14-GHz range using the Chebyshev function.

absorb τ_1 exactly and satisfy τ_2 with inequality. It is found by interpolation that

$$K = 0.98$$
$$\varepsilon^2 = 0.08 \quad (45)$$

will exactly absorb τ_1 and satisfy τ_2. The resulting reflection function is given by

$$s_{11}(\lambda) = \frac{1 + 1.02337\lambda + 2.46809\lambda^2 + 0.96756\lambda^3 + \lambda^4}{1 + 3.45815\lambda + 5.20164\lambda^2 + 2.53047\lambda^3 + \lambda^4}. \quad (46)$$

The synthesized circuit is shown in Fig. 12 with its response in Fig. 13.

In the same manner, from Table III, we can obtain the Chebyshev function parameters. The results are

$$K = 0.95$$
$$\varepsilon^2 = 0.01 \quad (47)$$

and

$$s_{11}(\lambda) = \frac{1 + 1.25754\lambda + 4.76677\lambda^2 + 3.31395\lambda^3 + 4.76677\lambda^4 + 1.25754\lambda^5 + \lambda^6}{1 + 2.80878\lambda + 7.92070\lambda^2 + 9.19022\lambda^3 + 7.92070\lambda^4 + 2.80878\lambda^5 + \lambda^6}. \quad (48)$$

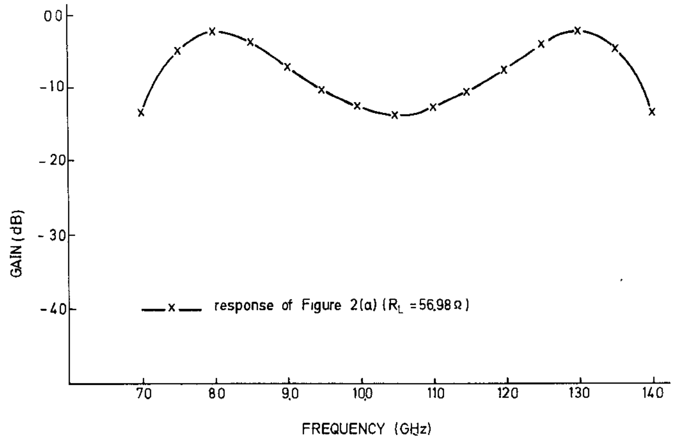

Fig. 11. Output circuit response of a chip FET amplifier.

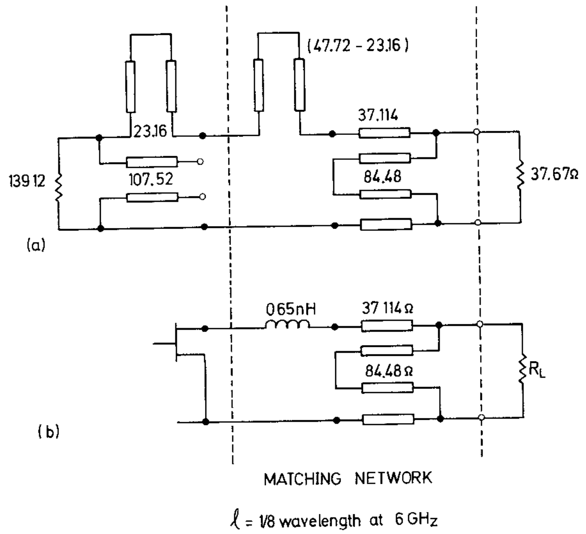

Fig. 12. Output matching network for a packaged FET in the 4–8-GHz range using the Butterworth function. (a) Original circuit. (b) Series shunted stub approximated by an inductor.

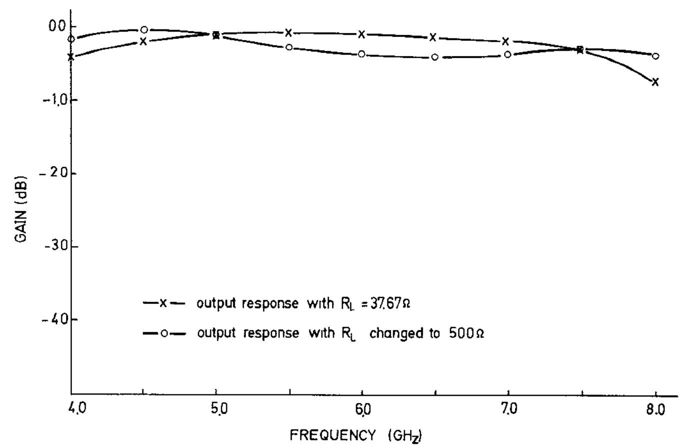

Fig. 13. Output circuit response of a packaged FET for the Butterworth case corresponding to Fig. 12.

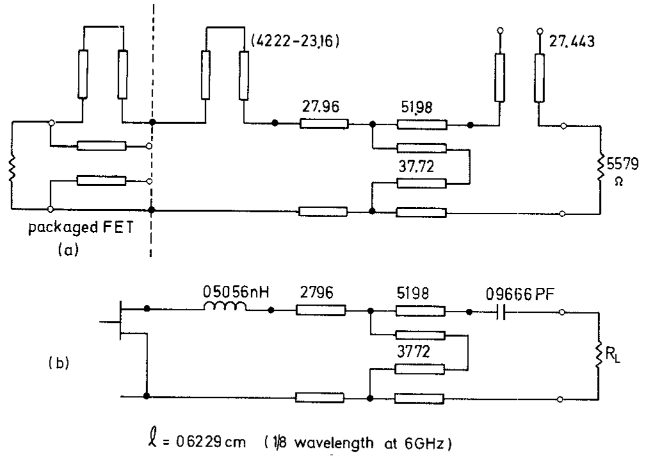

Fig. 14. Output matching network for a packaged FET in the 4–8-GHz range using the Chebyshev function. (a) Original circuit. (b) Series stubs approximated by lumped elements.

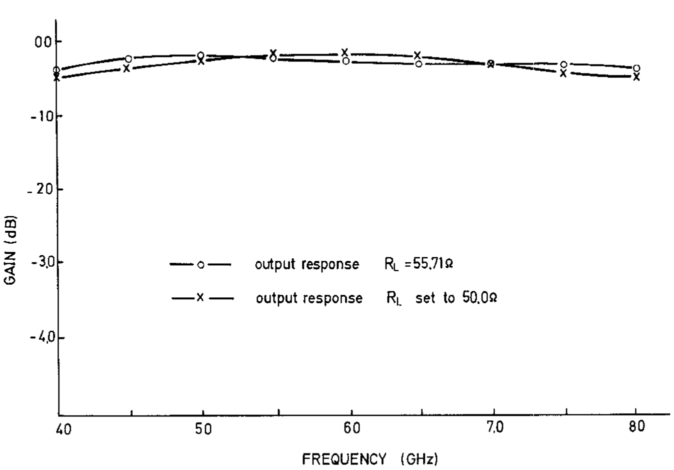

Fig. 15. Output circuit response of a packaged FET for the Chebyshev case corresponding to Fig. 14.

The synthesized circuit is shown in Fig. 14 in which the distributed to lumped approximations are also used due to practical realizability requirements. The output circuit response is shown in Fig. 15.

The matching of the input circuits of the transistors with required approximated tapered magnitude bandpass functions may be easily accomplished using one-eighth wavelength line structures [14], [15].

VI. Conclusions and Remarks

Characteristic functions to realize a new class of prototype transmission-line structures have been derived for both the Butterworth and the Chebyshev approximations. The new prototype is capable of reactance absorption and at the same time is able to adjust resistor ratios in a certain range due to shorted parallel stubs in the structure [9]. Since the line lengths are one-eighth the wavelength at the center of the band, it is possible to approximate open and shorted stubs by lumped capacitors and inductors, respectively. Designs are tabulated for certain configurations which are useful in broad-band matching of GaAs FET amplifiers [1]–[3].

The gain-bandwidth restrictions are investigated for two different reactive loads. The relations for two different Chebyshev functions with required configurations are compared with the optimal gain-bandwidth relations obtained for idealized gain functions in the distributed domain. The results can be applied, with minor modifications, to broad-band matching of series open-circuited stubs and series resonant circuits.

Acknowledgment

The authors would like to acknowledge the helpful discussions with Prof. H. J. Carlin and W. C. Petersen of Cornell University who ran some of the synthesis problems.

References

[1] R. S. Tucker, "Gain-bandwidth limitations of microwave transistor amplifiers," *IEEE Trans. Microwave Theory Tech.*, vol. MTT-21, May 1974.

[2] W. H. Ku, W. C. Petersen, and A. F. Podell, "New results on the design of broad-band microwave bipolar and FET amplifiers," in *Proc. IEEE GMTT Int. Symp.* (Atlanta, GA, June 12–14, 1974).

[3] W. H. Ku, M. E. Mokari-Bolhassan, W. C. Petersen, A. F. Podell, and B. R. Kendall, "Microwave octave-band GaAs FET amplifiers," in *Proc. Int. Microwave Symp.*, pp. 69–72 (May 12–14, 1975).

[4] E. Schwartz, "Broadband matching of resonant circuits and circulators," *IEEE Trans. Microwave Theory Tech.*, vol. MTT-16, Mar. 1968.

[5] T. M. Reeder and W. R. Sperry, "Broadband coupling to high-Q resonant loads," *IEEE Trans. Microwave Theory Tech.*, vol. MTT-20, July 1972.

[6] C. B. Sharpe, "A general Tchebycheff rational function," in *Proc. IRE*, pp. 454–457, Feb. 1954.

[7] D. Helman, "Tchebycheff approximations for amplitude and delay with rational functions," in *Proc. Symp. Modern Network Synthesis* (Polytechnic Institute of Brooklyn, NY), vol. 5, pp. 385–402, Apr. 1955.

[8] E. M. T. Jones, "Synthesis of wide-band microwave filters to have prescribed insertion loss," in *1956 IRE Convention Record*, pt. V, pp. 119–128.

[9] H. J. Carlin and W. Kohler, "Direct synthesis of band-pass transmission line structures," *IEEE Trans. Microwave Theory Tech.*, vol. MTT-13, May 1965.

[10] H. J. Riblet, "The application of a new class of equal ripple functions to some familiar transmission line problems," *IEEE Trans. Microwave Theory Tech.*, vol. MTT-13, pp. 415–421, July 1964.

[11] H. Ozaki and J. Ishii, "Synthesis of transmission line networks and the design of UHF filters," *IRE Trans. Circuit Theory*, vol. CT-2, pp. 325–336, Dec. 1955.

[12] R. Levy, "Synthesis of mixed lumped and distributed impedance-transforming filters," *IEEE Trans. Microwave Theory Tech.*, vol. MTT-20, Mar. 1972.

[13] R. M. Fano, "Theoretical limitations on the broad-band matching of arbitrary impedances," *J. Franklin Institute*, vol. 249, pp. 57–83, Jan. 1950, also pp. 138–154, Feb. 1950.

[14] D. C. Youla, "A new theory of broadband matching," *IEEE Trans. Circuit Theory*, vol. CT-11, pp. 30–50, Mar. 1964.

[15] M. E. Mokari-Bolhassan and W. H. Ku, "Broadband matching of complex impedances with lossless transmission line structures," presented at the 5th Iranian Conf. Electrical Engineering, Oct. 27–30, 1975.

[16] ——, "Tapered magnitude bandpass distributed network transfer functions," to be published in *Int. J. Circuit Theory and Applications.*